Carbohydrate Polymers 98 (2013) 189–198

Contents lists available at SciVerse ScienceDirect

Carbohydrate Polymers

journal homepage: www.elsevier.com/locate/carbpol

Carbon nanotubes in blends of polycaprolactone/thermoplastic starch

Ata Taghizadeh, Basil D. Favis*

CREPEC, Department of Chemical Engineering, École Polytechnique de Montréal, 2900 Édouard Montpetit, P.O. Box 6079, Station Centre-Ville, Montréal, Québec, Canada H3C 3A7

ARTICLE INFO

Article history:
Received 19 February 2013
Received in revised form 9 May 2013
Accepted 13 May 2013
Available online 31 May 2013

Keywords:
Polycaprolactone (PCL)
Thermoplastic starch (TPS)
Carbon nanotubes
Localization
Morphology
Interface

ABSTRACT

Despite the importance of polymer–polymer multiphase systems, very little work has been carried out on the preferred localization of solid inclusions in such multiphase systems. In this work, carbon nanotubes (CNT) are dispersed with polycaprolactone (PCL) and thermoplastic starch (TPS) at several CNT contents via a combined solution/twin-screw extrusion melt mixing method. A PCL/CNT masterbatch was first prepared and then blended with 20 wt% TPS. Transmission and scanning electron microscopy images reveal a CNT localization principally in the TPS phase and partly at the PCL/TPS interface, with no further change by annealing. This indicates a strong driving force for the CNTs toward TPS. Young's model predicts that the nanotubes should be located at the interface. X-ray photoelectron spectroscopy (XPS) of extracted CNTs quantitatively confirms an encapsulation by TPS and reveals a covalent bonding of CNTs with thermoplastic starch. It appears likely that the nanotubes migrate to the interface, react with TPS and then are subsequently drawn into the low viscosity TPS phase. In a low shear rate/low shear stress internal mixer the nanotubes are found both in the PCL phase and at the PCL/TPS interface and have not completed the transit to the TPS phase. This latter result indicates the importance of choosing appropriate processing conditions in order to minimize kinetic effects. The addition of CNTs to PCL results in an increase in the crystallization temperature and a decrease in the percent crystallinity confirming the heterogeneous nucleating effect of the nanotubes. Finally, DMA analysis reveals a dramatic decrease in the starch rich phase transition temperature (~26 °C), for the system with nanotubes located in the TPS phase.

1. Introduction

Bioplastics include polymers that are biodegradable, e.g. polycaprolactone (PCL), or biobased, such as biobased polyethylene, or both such as thermoplastic starch (TPS) and PHAs (Queiroz & Collares-Queiroz, 2009). Despite their high annual growth rates, most bioplastics suffer from their inability to cover a broad range of mechanical properties in comparison with the commodity plastics; e.g. PLA or PHB show high modulus, but very low elongation at breaks; PCL demonstrates excellent ductility but suffers from low modulus. Among them, thermoplastic starch (TPS), a widely available biobased material with reasonable cost and excellent biodegradation properties, has been significantly studied (Averous, 2004). Thermoplastic starch can easily flow at high temperatures and be melt processed in a similar fashion to other thermoplastic polymers. The major drawback of TPS, however, is its susceptibility to humidity and weak mechanical properties which generally limits its use in pure form and requires it to be blended with other polymers.

PCL has been used in soft compostable packaging (Averous, 2004) as well as in tissue engineering applications (Bajgai et al., 2008). It has hydrophobic characteristics and shows excellent ductility. However, it is a petroleum based polymer with a low degradation rate and several copolymers such as DL-lactide or glycolide have been incorporated in the structure of PCL to improve its degradation properties (Nair & Laurencin, 2007). Additionally, the degradation rate of polycaprolactone has been shown to be significantly improved in presence of starch (Shin, Lee, Shin, Balakrishnan, & Narayan, 2004). The blending of PCL with thermoplastic starch will increase the biobased portion/biodegradation rate of the PCL products. Several groups have already studied blends of PCL/TPS and have reported a complete immiscibility between the two polymers. Averous, Moro, Dole and Fringant (2000) have shown complete incompatibility of the two pairs based on T_g curves, however, significant improvements in the mechanical properties of TPS were observed. In a recent work in this laboratory (Li & Favis, 2010), the incorporation of TPS in a PCL matrix was shown to result in very fine and stable morphologies. These TPS/PCL blends demonstrated a high ductility at values as high as 50 wt% TPS and a corresponding drop in the modulus compared to neat PCL. This level of morphology control can be used as a starting point to evaluate the effect of the incorporation of solid nanoinclusions

* Corresponding author. Tel.: +1 514 340 4711x4527; fax: +1 514 340 4159.
E-mail address: basil.favis@polymtl.ca (B.D. Favis).

0144-8617/$ – see front matter © 2013 Elsevier Ltd. All rights reserved.
http://dx.doi.org/10.1016/j.carbpol.2013.05.024

as a route toward higher performance materials. Owing to the superior mechanical, electrical, magnetic, optical and thermal properties of carbon nanotubes (CNT), they offer the potential to generate novel materials when properly dispersed in a polymer resin (Moniruzzaman & Winey, 2006). In recent years carbon nanotubes have been successfully added to polymer blends improving the morphology and/or mechanical properties. However, any possible improvement introduced to the polymer blends is highly dependent on the level of dispersion and their localization. There are two factors influencing the nanoparticles localization: thermodynamics and kinetic effects. Ideally, CNTs will migrate to the phase with which they have the lowest interfacial tension in order to minimize the free energy of the system (thermodynamic effect) (Fenouillot, Cassagnau, & Majeste, 2009). This will lead to a stable dispersion which is expected to remain unchanged even by further processing. Goeldel, Kasaliwal and Poetschke (2009) showed that nanotubes can migrate to their thermodynamically favorable phase (i.e. PC in PC/SAN blends), irrespective of the mixing strategy. Several authors have tried to predict the localization of nanoparticles in polymer blends by calculating the interfacial tensions between the blend components (Elias, Fenouillot, Majeste, & Cassagnau, 2007; Katada, Buys, Tominaga, Asai, & Sumita, 2005). However, the evaluation of the interfacial tensions of polymers/solid inclusions is complex and has not been examined significantly in the literature. A rough estimation of the interfacial tensions can limit the ability to predict the localization in all cases (Wu et al., 2011).

Another determining factor related to the localization of nanofillers in polymeric systems is kinetics. Kinetics include processing parameters such as mixing sequence and shear rate as well as the viscosity, temperature, or even the shape of the nanofiller (Fenouillot et al., 2009; Goeldel, Kasaliwal, Poetschke, & Heinrich, 2012). Each of these may suppress the migration of the nanofillers to the thermodynamically stable state of dispersion, for example, an increased viscosity of PCL in PCL/PLA blends (Wu et al., 2011) or PMMA in PMMA/PP blends (Feng, Chan, & Li, 2003).

There are several methods for the dispersion of nanotubes in polymer matrix. Generally, the solvent dissolution method is shown to be one of the most efficient methods to disperse nanotubes in polymers but is mostly applicable at the laboratory scale (Grady, 2010). Melt mixing is the preferred method in spite of its lower comparative efficacy (Bose, Bhattacharyya, Bondre, Kulkarni, & Potschke, 2008; Goeldel et al., 2012). A combination of these methods may result in a high level of dispersion without damaging the nanotubes as is observed in masterbatch-type processes (Abbasi, Carreau, & Derdouri, 2010). It is expected that kinetic effects will be different depending on the type of mixing equipment with their different flow fields and intensity or processing times and hence, the localization of the nanoparticles may be potentially different in different mixing equipments (Breuer & Sundararaj, 2004).

The objective of this work is to investigate the localization of carbon nanotubes in blends of thermoplastic starch/polycaprolactone. Two melt blending operations will be examined. The observed localization of carbon nanotubes in the multiphase system will be compared to predictive models and the relative role of thermodynamic and kinetic effects will be addressed. The influence of carbon nanotubes on the morphology of the blend will be studied. Finally, the influence of carbon nanotubes on the physical properties of the material will be assessed.

2. Experimental

2.1. Materials

The native wheat starch and glycerol were obtained from ADM and Labmat, respectively. The wheat starch was composed of 25% amylose and 75% amylopectin. The glycerol was pure at 99.5% and contained 0.5% water. Polycaprolactone (PCL), CAPA 6500, was supplied by Solvay Chemicals. Capa6500 has a molecular weight of 50,000 g mol^{-1} and a MFI of 7.0 (g per 10 min, 160 °C). Surface modified multiwall carbon nanotubes (NC3101) were purchased from Nanocyl Co. The average diameter and length of CNTs were 9.5 nm and 1.5 μm, respectively with a carbon purity of greater than 95%. The carboxylic acid surface modification was evaluated by XPS to be ~4%.

2.2. PCL/CNT preparation

A PCL–CNT masterbatch was first prepared at high CNT loadings (9–11 wt%) through a solution casting method at room temperature. Nanotubes were dispersed in THF for 1 h via ultrasonication. Then the PCL/THF solution was added to CNT solution and ultrasonication continued for 1 h more. An antisolvent was added to the solution at the end and precipitated PCL and CNT were dried in the vacuum oven at 35 °C for a week. The nanotubes wt% in the masterbatches was determined by TGA (TGA Q500, TA Universal).

2.3. Blend preparation

2.3.1. Twin-screw

The PCL/CNT masterbatch then went through two different methods of preparation. In method one, TPS/PCL blends were prepared in a twin screw extruder via an established method in this laboratory (Favis, Rodriguez-Gonzalez, & Ramsay, 2003; Favis, Rodriguez-Gonzalez, & Ramsay, 2005) which consists of a single screw extruder (SSE) connected midway to a co-rotating twin screw extruder (TSE). The starch/glycerol/water suspension was fed to the TSE in which native starch was gelatinized and plasticized and the water was extracted before molten PCL/CNT are fed from the SSE to midway on the TSE. The TPS slurry was formulated in a way that the final TPS consists of 36 wt% glycerol. The compositions were all constant at PCL/TPS: 80/20 wt%. The screw speed was set at 100 rpm and the mixing zone temperatures were fixed at 145 °C. In order to obtain the CNT content of the blends, in each step thermogravimetric analyses (TGA) tests were conducted. CNT contents were 0.5 and 1 wt% based on the whole blend.

2.3.2. Brabender

In a second blending method, pure TPS was obtained via the above method in a twin screw extruder (Favis et al., 2003, 2005). The blend with PCL was then prepared via an internal mixer (Brabender Plasticorder). The rotor speed was set at 100 rpm and the processing temperature was at 145 °C. The master batch and neat PCL were then first fed to an internal mixer and after reaching plateau of the torque, thermoplastic starch (TPS) was added to the chamber. The compositions were all constant in PCL/TPS: 80/20 wt%. CNT contents were 0.5, 1 and 2 wt% based on the whole blend.

In order to prepare the samples for further characterization tests, the samples of both methods were compression molded at 145 °C. In order to be able to easily remove the samples, two Teflon sheets were inserted between metal plaques and molds. The total molding process time took 8 min under a nitrogen atmosphere after which it was quenched in a cold press to freeze-in the morphology.

Quiescent annealing was further conducted on some selected samples of both processing methods at 145 °C for up to 60 min.

2.4. Rheological characteristics

Rheological characterizations of the thermoplastic starch and PCL were performed in oscillation mode using a MCR-301 strain controlled rheometer from *Anton Paar*. The experiments were

Table 1
Surface tension parameters of different incorporated materials.

	γ_d (mN/m)	γ_p (mN/m)	γ (mN/m)
PCL			
@ 23 °C	42	10.2	52.3
@ 145 °C[a]	36.4	8.8	45.2
TPS			
@ 23 °C	25.4	7.61	33.01
@ 145 °C	19.9	6	25.9
CNT			
@ 145 °C	18.4	26.9	45.3

[a] Surface tensions calculated at 145 °C ($d\sigma/dT$: −0.058 mN/(mK)) (Cava et al., 2007).

conducted in parallel plate geometry. First a stress sweep test was run to define the region of linear viscoelasticity. Then a frequency sweep test was conducted on the samples from 0.1 rad/s to 200 rad/s at 145 °C and 165 °C. Another stress sweep test was run in a constant shear rate of 52 rad/s.

2.5. Scanning and transmission electron microscopy

In order to observe the localization of the nanotubes, scanning (SEM) and transmission (TEM) imaging were conducted on the samples. Microtoming, followed by platinum coating was carried out on certain samples. The prepared samples were then subjected to SEM imaging to observe the nanotubes on the surface. In order to obtain the morphology of the blends, the as-prepared samples were microtomed and then the TPS phase was extracted by HCl (6 N). The prepared surfaces were gold coated for further microscopic investigations. Image analyses were performed on the sample images to obtain both number and volume average diameters. The microscope was a Jeol JSM 7600TFE Scanning Electron Microscope (SEM) operated at a voltage of 2 kV. Ultramicrotoming followed by TEM imaging (Jeol JSM 2100F, operating at 200 kV) was used on some selected samples to have a magnified view of the nanotubes in the blends on the prepared ultrathin samples. The micrographs were manually digitized using a digitizing table from Wacom and SigmaScan v.5 software. In order to determine the phases in both SEM and TEM images, some selected samples were subjected to selective extraction and based on those images the phases are identified.

2.6. Surface tension measurements

The surface tensions of thermoplastic starch and polycaprolactone were measured by the sessile drop method with probe liquids. The details of the contact angle measurement technique can be found elsewhere (Kwok & Neumann, 1999). The obtained data are represented in Table 1. Comparing the obtained values with other reported data, it is found that the surface tensions obtained for TPS and PCL are in agreement with the literature (Averous & Boquillon, 2004; Wu et al., 2011). The surface tension data for carbon nanotubes are obtained from the work of Nuriel, Liu, Barber and Wagner (2005) which reports the highest polarity values (Goeldel, Marmur, Kasaliwal, Poetschke, & Heinrich, 2011) and has been frequently used in the literature for carbon nanotubes of similar size and structure (Potschke, Pegel, Claes, & Bonduel, 2008; Wu et al., 2011). Interfacial tension was calculated based on geometric-mean:

$$\gamma_{xy} = \gamma_x + \gamma_y - 2[(\gamma_x^d \gamma_y^d)^{1/2} + (\gamma_x^p \gamma_y^p)^{1/2}] \quad (1)$$

and harmonic-mean equations (Wu, 1987):

$$\gamma_{xy} = \gamma_x + \gamma_y - 4\left[\frac{\gamma_x^d \gamma_y^d}{\gamma_x^d + \gamma_y^d} + \frac{\gamma_x^p \gamma_y^p}{\gamma_x^p + \gamma_y^p}\right] \quad (2)$$

Table 2
Interfacial energies for all possible different interfaces.

	Interfacial energy according to harmonic mean equation (mN/m)	Interfacial energy according to geometric mean equation (mN/m)
PCL/TPS	5.4	2.7
PCL/CNT	15.1	8
TPS/CNT	13.3	7.5

where γ_x is the surface tension of material x and its two components, are dispersive γ_x^d and polar γ_x^p, and γ_{xy} is the interfacial tension between phase x and phase y (Table 2).

2.7. X-ray photoelectron spectroscopy (XPS)

XPS was used in order to quantitatively verify the nature of the encapsulating polymer and its interaction on the carbon nanotube surface. In order to run the XPS test on the nanotubes surface, PCL was removed by THF for one week, followed by TPS extraction by 6 N HCl for the same time period. This procedure was repeated twice in order to extract any polymer left on the surface of the nanotubes. The nanotubes were then separated centrifugally from the solution. The dried extracted nanotubes along with pure nanotubes were scanned by XPS. X-ray Photoelectron Spectroscopy (XPS) was conducted on a (VG ESCALAB 3 MKII) spectrometer with Mg-Kα ray source. Survey scans of 100 eV pass energy were used to identify initially all components followed by high resolution individual scans using a pass energy of 20 eV. The surface elemental stoichiometry was obtained from the ratios of peak areas corrected with the Wagner sensitivity factors and Shirley background subtraction.

2.8. Differential scanning calorimetry (DSC)

In order to obtain the effect of nanofillers on the crystallinity of PCL, a differential scanning calorimetry instrument (DSC Q1000, TA instruments) was used at a heating–cooling rate of ±10 °C min^{-1} between −30 and 80 °C with an empty sample pan as the reference. The blends were weighed (10–15 mg) and then sealed. The calorimetric data extracted from these tests was determined using Universal Analysis® software.

2.9. Dynamic mechanical analyses (DMA)

Dynamic mechanical properties were measured using a TA dynamic mechanical analyzer (TA Instruments, DMA 2980). The temperature was increased from −100 °C to 40 °C, with a heating rate of 3 °C min^{-1}. The frequency was 1 Hz, and the oscillation amplitude was 30 μm. The measurements were carried out using the dual cantilever clamp mode.

3. Results and discussion

3.1. Morphology and localization of carbon nanotubes in TPS/PCL blends prepared by twin-screw extrusion

SEM images of PCL/TPS blends prepared by twin-screw extrusion are shown in Fig. 1. The carbon nanotubes can be clearly identified as white spots and it can be seen that the nanotubes are located in the TPS phase and at the interface. TEM microscopy was also conducted on selected samples and Fig. 2 confirms the localization of the nanotubes mainly in the bulk of the TPS phase and a small portion at the interface. Annealing selected samples was carried out in order to determine the morphological stability. The samples after annealing demonstrated the same morphological state as seen in Figs. 1 and 2. The strong driving force of the

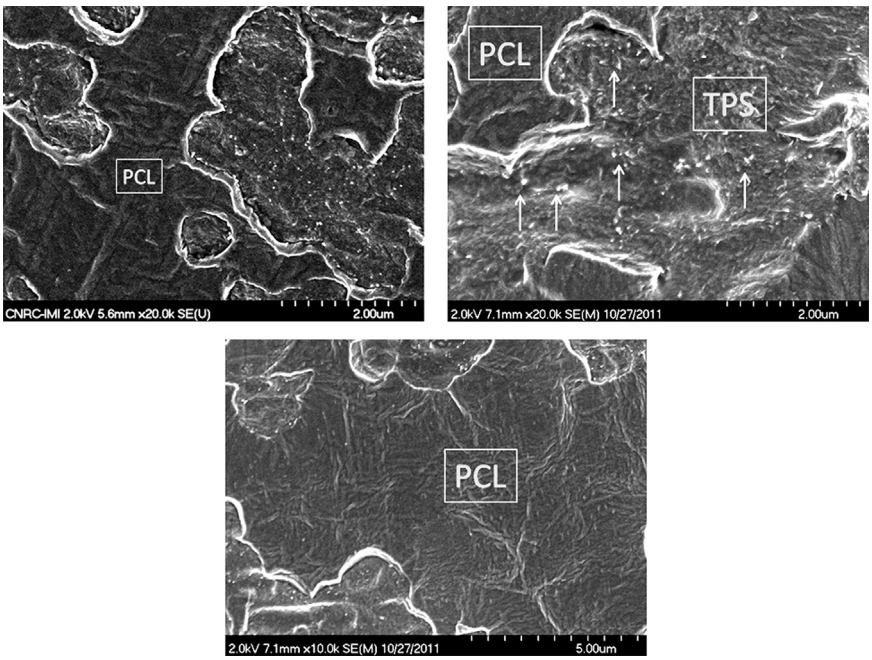

Fig. 1. SEM images of blends of PCL/TPS 80/20 wt% with 1 wt% CNT prepared by twin screw extrusion.

nanotubes for TPS is considered to be even more dramatic when it is considered that, in the blending process, the nanotubes were first introduced into the PCL phase. During the blending process the nanotubes clearly migrate from the PCL phase to the interface with a significant proportion penetrating into the TPS phase.

From a thermodynamic standpoint, the localization of solid inclusions is controlled by the minimization of the free energy of the system (Goeldel et al., 2009; Potschke et al., 2008). The thermodynamic equilibrium for the localization of a solid inclusion can be estimated by Young's equation (Eq. (3)) (Sumita, Sakata, Asai, Miyasaka, & Nakagawa, 1991):

$$\omega = \frac{\gamma_{CNT-B} - \gamma_{CNT-A}}{\gamma_{A-B}} \quad (3)$$

where γ_{x-y} is the interfacial tension between component x and y and ω is the wetting coefficient. If $\omega > 1$, then the CNT will migrate to phase A, if $\omega < -1$ it will be dispersed in B, but if $-1 < \omega < 1$, the CNT will mainly go to the interface. Assigning A as PCL and B as TPS and calculating the wetting coefficient based on the data obtained in Table 2, result in −0.33 and 0.18 for harmonic-mean and geometric-mean equations, respectively. Consequently, both the harmonic and geometric mean approaches to estimate interfacial tension and subsequently the wetting coefficient results in the prediction that the nanotubes should be located at the interface. However, the above data for twin-screw extrusion shows that the nanotubes are not only at the interface but also principally in the bulk of the TPS phase.

The morphology and mechanical properties of PCL/TPS blends have been studied previously in this laboratory (Li & Favis, 2010). That study points to a high level of compatibility between the TPS and the PCL and it shows that: the quiescent annealing data displays a high stability of the TPS phase in PCL; dynamic mechanical analyses point to the presence of a specific interaction between the PCL and the TPS; and FT-IR spectroscopy shows the presence of a hydrogen bonding interaction between the carbonyl groups of the PCL and the hydroxyl groups on the starch. In this work, adding nanotubes to the blend did not result in any change in the TPS phase size or morphology as is reported in Table 3. Typically solid inclusions may affect the morphology of blends by changing the phase viscosity and/or the nature of the interface (Fenouillot et al., 2009). In this work, it appears that the high level of compatibility between PCL and TPS dominates the morphology and any change to the viscosity of the TPS phase through the addition of nanotubes appears to be a minor effect. It should also be noted that the elongational flow component of twin-screw extrusion mixing is particularly effective at reducing the dispersed phase size and as such the phase size tends to demonstrate a reduced dependence on viscosity ratio (Favis, 2000).

3.1.1. XPS analysis of carbon nanotube surface

XPS analyses were conducted on samples that had been selectively extracted for both PCL and TPS in order to quantitatively confirm the encapsulating phase around the nanotubes and also evaluate the type of interaction occurring at the nanotube surface. The surface compositions of the nanotubes before and after blending in the twin-screw extruder were examined. The survey spectra overlay of pure and extracted carbon nanotubes surfaces are shown in Fig. 3. The significant increase of atomic oxygen from 8% to 23% is clearly observed on this overlay indicating the clear preferential encapsulation of nanotubes by one of the phases. The high resolution spectra of the carbon region for pure and extracted nanotubes are shown in Fig. 4. The carbon region curves were fitted with six symmetric components identifying the different carbon functional groups present on the surface of the nanotubes. Components C1

Table 3
Number and volume average diameter size of TPS phase in the PCL/TPS 80/20 wt% blends with different carbon nanotube contents prepared by extrusion and internal mixing.

	d_n(μm)	d_v(μm)
PCL/TPS[a]	1.4	1.9
PCL/TPS + 0.5 wt% CNT[a]	1.2	1.6
PCL/TPS + 1 wt% CNT[a]	1.3	1.7
PCL/TPS[b]	3	3.6
PCL/TPS + 0.5 wt% CNT[b]	1.1	1.7
PCL/TPS + 1 wt% CNT[b]	0.7	1.6
PCL/TPS + 2 wt% CNT[b]	0.7	1.7

[a] Prepared by extrusion.
[b] Prepared by internal mixing.

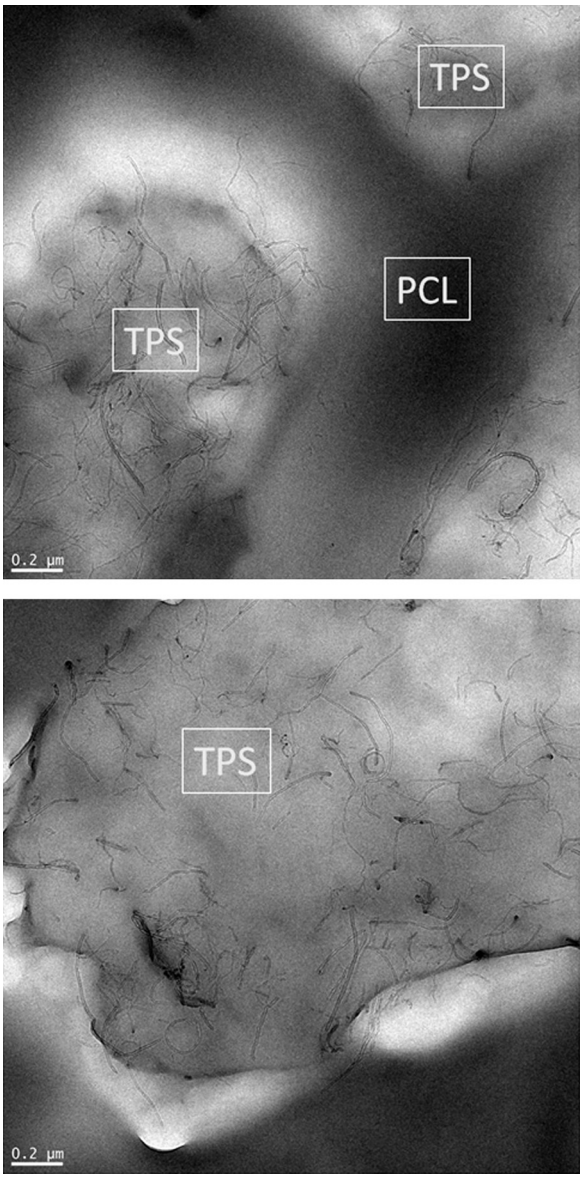

Fig. 2. TEM images of blends of PCL/TPS 80/20 wt% with 1 wt% CNT prepared by twin screw extrusion.

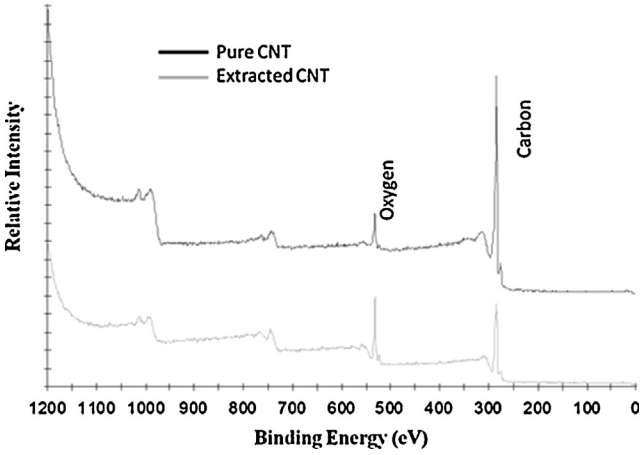

Fig. 3. XPS survey spectra of fresh and extracted (after 2 weeks of solvent extraction) nanotubes. The curves were offset for clarity.

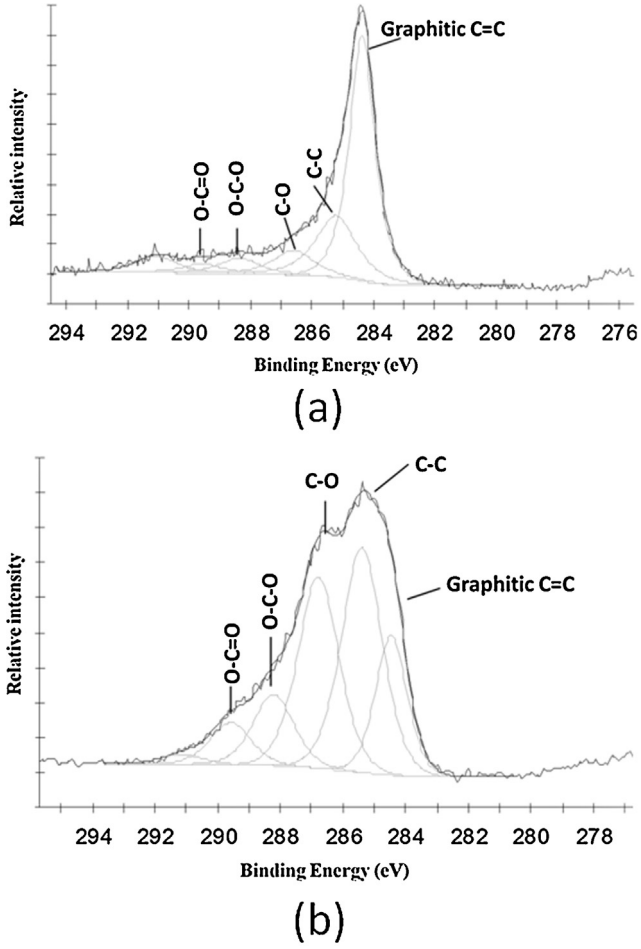

Fig. 4. Narrow scan spectra of carbon region for: (a) fresh nanotubes; (b) extracted nanotubes.

and C2 at a binding energy (B.E.) of 284.4 eV and 285.3 eV, respectively, indicate sp^2 graphitic carbon, and sp^3 carbon plus sp^2 carbon defects. C3 at a B.E. of 286.5 eV indicates C—O and C—O—C groups, while C4 at 288.4 eV indicates the presence of O—C—O groups (Luong et al., 2005). The relative intensity of the carbon functional groups found on the surface of the CNT in the extracted samples is significantly different from that observed on the pure nanotubes. A comparative decrease in intensity of sp^2 graphitic carbon and simultaneous increase of carbon–oxygen functional groups on the surface of extracted nanotubes compared to the pure ones allows for the identification of the encapsulating phase. By considering the ratios of C3 (C—O) and C4 (O—C—O) over C2 (sp^3 C—C and sp^2 carbon defects) on the extracted samples, C3/C2 is increased compared to that on the pure CNT by a factor of 114% while C4/C2 is increased by a factor of 24%. In other words, the increase of C—O functions is close to five times the increase of O—C—O functions (Table 4). Since the ratio of C—O to O—C—O functions in a model starch molecule is 5–1, this confirms the encapsulation of nanotubes by starch chains. The ability of starch to remain on the carbon

Table 4
Relative functional groups increase on the carbon nanotube walls before and after extrusion process.

	C3/C2 (C—O/C—C)	C4/C2 (O—C—O/C—C)
Pure CNT	0.399	0.255
Extracted CNT	0.854	0.318
Total increase	114%	24%

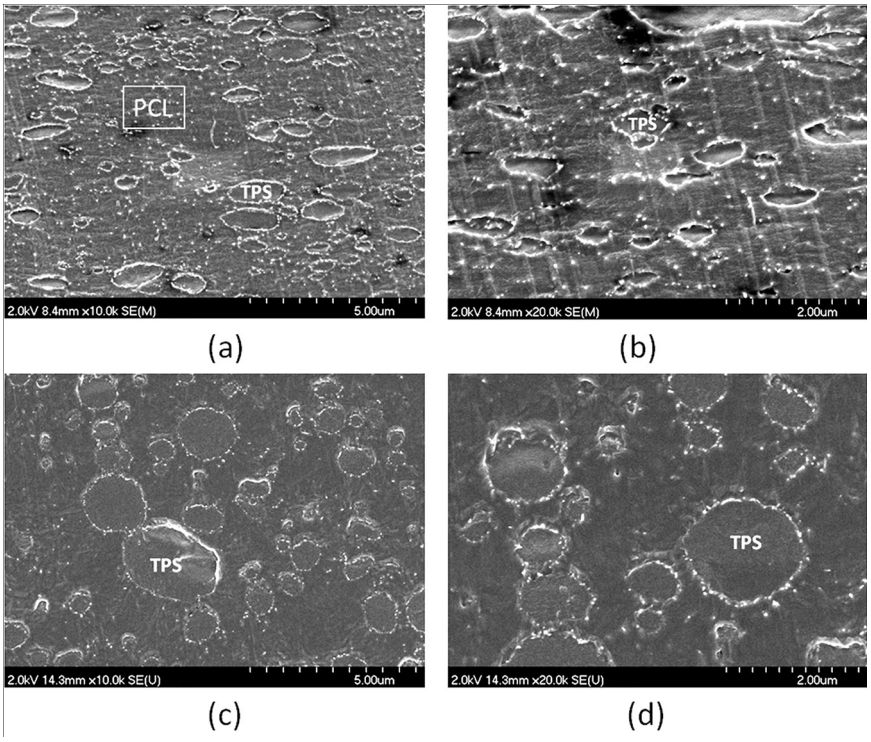

Fig. 5. SEM images of blends of PCL/TPS 80/20 wt% with 2 wt% carbon nanotube prepared by internal mixer: (a) and (b) frozen morphology after process; (c) and (d) annealed samples for 1 h at 145 °C.

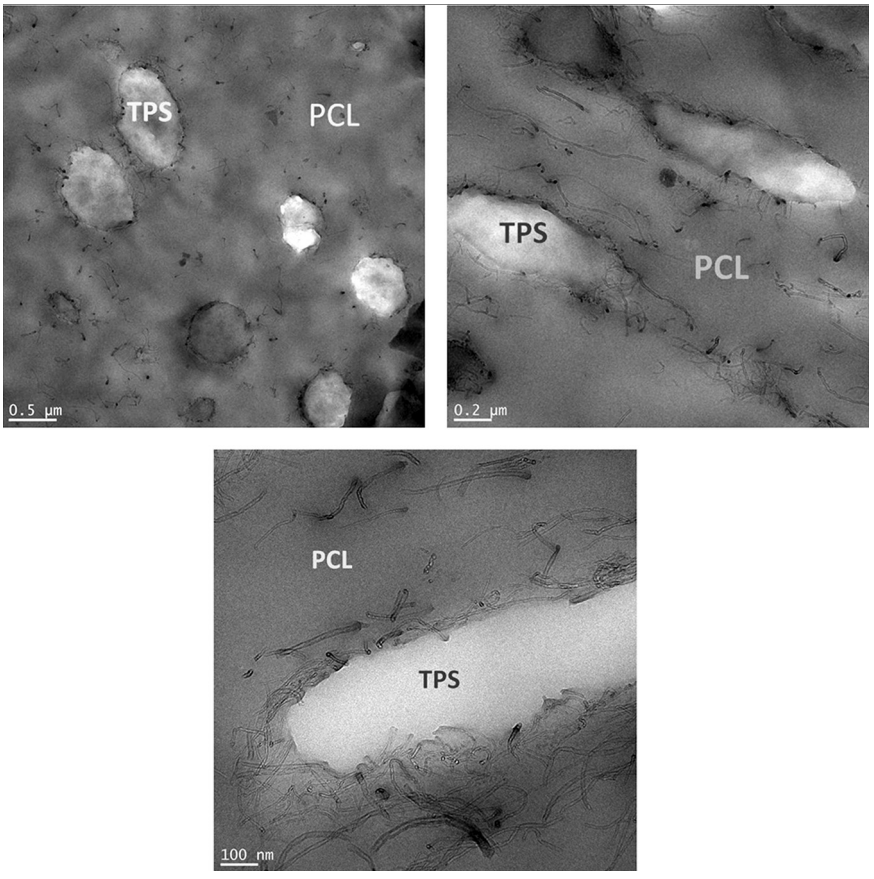

Fig. 6. TEM images of blends of PCL/TPS 80/20 wt% with 2 wt% carbon nanotube prepared by internal mixer.

nanotube surface even after multiple extractions and two weeks of solubilization is strongly indicative of the formation of a covalent bond between the carboxylic acid groups on the nanotube surface and the OH of the TPS. Such interactions between starch and carbon nanotubes have been shown by other authors as well (Angellier, Molina-Boisseau, Dole, & Dufresne, 2006; Ma, Yu, & Wang, 2008).

3.1.2. Physical model

Dynamic mixing allows for the nanotubes to move through the PCL phase. Once in contact with the interface, the nanotubes localize there in a stable fashion in order to minimize the overall surface free energy. At the interface a reaction occurs between the carboxylic acid groups of the nanotube and the alcohol groups of the starch. Following this reaction and the formation of a TPS encapsulating layer around the nanotube, the carbon nanotubes are drawn into the thermoplastic starch dispersed phase.

3.2. TPS/PCL/carbon nanotubes localization in an alternative process (internal mixer)

The twin screw extrusion led to the localization of the carbon nanotubes principally in the TPS phase. However, as explained earlier, this localization may be impeded in some processes due to kinetic effects. In order to assess the influence of a different processing technique on carbon nanotube localization, an internal mixer was used. Since the internal mixer imposes a predominantly shear flow field, its influence on the localization process will be interesting to examine. In this method, a similar procedure was applied as in twin screw extrusion.

Although the sequence of CNT addition was maintained, i.e. CNT is fed to the system through the PCL phase, it is observed that the localization of CNTs in the internal mixer is totally different from the previous twin-screw extrusion method. In the internal mixer, the nanotubes do not migrate to the TPS phase but rather remain in the PCL phase and at the PCL/TPS interface (Figs. 5 and 6). Annealing the samples results in the nanotubes moving more toward the interface and the TPS bulk phase remains completely CNT-free.

In the twin screw extruder and internal mixer, two different shear fields exist. The internal mixer has been generally considered to have a predominantly simple shear flow between the sample and the walls of the chamber (Bousmina, Ait-Kadi, & Faisant, 1999). However, in a twin screw extruder, in addition to shear flow, strong elongational fields exist as well (Favis, 2000).

The viscosity-shear rate variation for TPS denotes a significant shear thinning behavior (Fig. 7). Comparing the apparent shear rates in the two mixing procedures; it is observed that with 100 rpm in the twin screw extruder, the apparent shear rate at the die, where the pressure increases and filling factor is ~1, is around 88/s (Clark, Geramita, & Baker, 1999; Shahbikian, 2010). Note that during twin-screw extrusion mixing it is expected that the shear rates in the high intensity mixing zones would even be significantly higher, but it is virtually impossible to estimate with any accuracy. On the other hand, at 100 rpm of the internal mixer the apparent shear rate is ~52/s (Bousmina et al., 1999). Thus, the TPS viscosity is expected to increase dramatically in the internal mixer shear field. In addition to shear fields, TPS has been shown to have a significant shear thinning nature in elongational flow fields as well (Valle, Vergnes, & Lourdin, 2007), which will act as another factor for further reducing the viscosity of TPS in the twin screw extrusion process. The applied shear stress is also expected to vary and increase to very high amounts in the extruder due to the pressure variation as a result of the different kneading elements. Additionally, preliminary laboratory tests have shown that, contrary to PCL, TPS is very sensitive to shear stress (not shown here). Hence, it is expected for TPS to have a much lower actual viscosity in the twin-screw extruder than in the internal mixer. It is thus believed that this increase of TPS viscosity

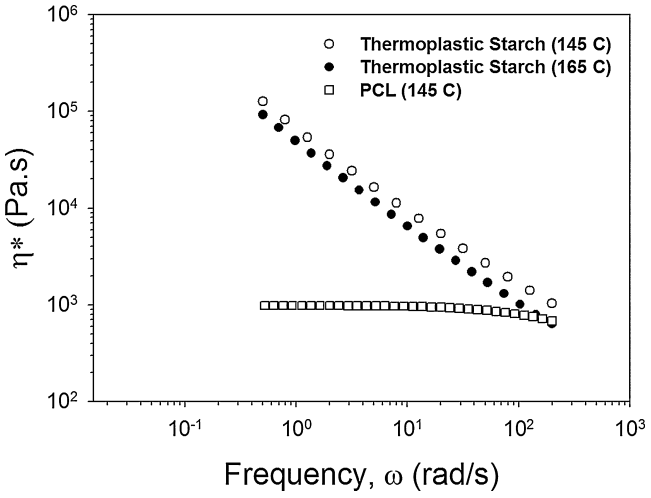

Fig. 7. Variation of complex viscosity with frequency for TPS and PCL at different processing temperatures.

in the internal mixer does not allow the reacted nanotubes to be drawn into the TPS phase and they remain at the interface. This is confirmed by carrying out the internal mixing at a higher temperature. Fig. 8 clearly shows a change in localization in the higher temperature process and the nanotubes have been able to partly penetrate into the TPS phase due to the decrease in TPS viscosity.

Thus, in shear sensitive materials such as TPS where the melt viscosity, as well as the flow field, can be significantly changed by processing technique and parameters, the localization of the nanofillers can be subjected to change. This localization may not necessarily be the thermodynamically favorable state of dispersion and therefore the nanotube localization may be subjected to change by further processing under different processing conditions in order to reach the equilibrium state of dispersion.

The TPS dispersed phase size is significantly influenced by the high concentration of nanotubes at the PCL/TPS interface during mixing with the internal mixer. This effect is clearly observed in Fig. 9. With the incorporation of 0.5 wt% nanotubes, the TPS droplet size reduces by half (Table 3). This decrease continues for d_n up to 1 wt% CNT after which it reaches a plateau. It appears, in the case of the internal mixer, that the localization of the nanotubes at the PCL/TPS interface generates a physical barrier for the dispersed TPS phase coalescence, thus resulting in a significant reduction of phase size. On the other hand, increasing the viscosity of the matrix will increase the capillary number resulting in a smaller droplet size (Favis, 2000).

3.3. Differential scanning calorimetry (DSC)

Polycaprolactone (PCL) is a semicrystalline polymer with a crystallinity of around 40%. As shown in Table 5, the addition of TPS results in the increase of the PCL crystallization temperature which is believed to be due to the heterogeneous nucleating effect of TPS, however, the percent crystallinity remains almost unchanged in both processes. It has been shown that natural polymers such as starch can act as a nucleating agent and promote crystallization kinetics, but the final small size of crystals and their low degree of perfection might even decrease the enthalpy of melting and consequently the crystallinity percentage (Ciardelli et al., 2005). Nanotubes are also materials which can act as strong nucleating agents in polymers and change the crystallization type and structure (Grady, 2012). Table 5 reveals that all of the CNT-incorporated blends of PCL/TPS show a higher T_c than for the neat blend of PCL/TPS which is due to the heterogeneous nucleating effect of

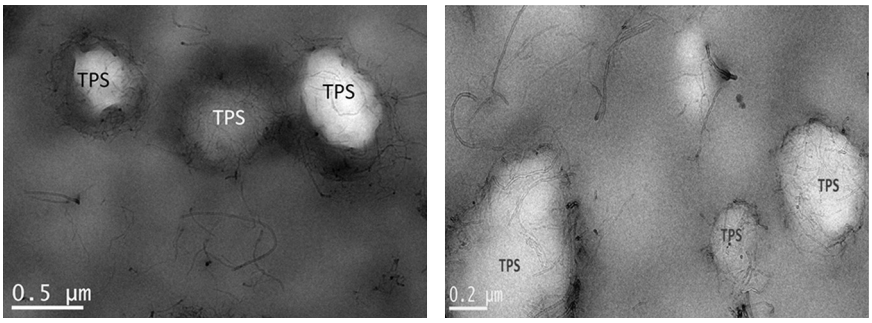

Fig. 8. TEM images of blends of PCL/TPS 80/20 wt% with 2 wt% carbon nanotube prepared by internal mixer at 165 °C.

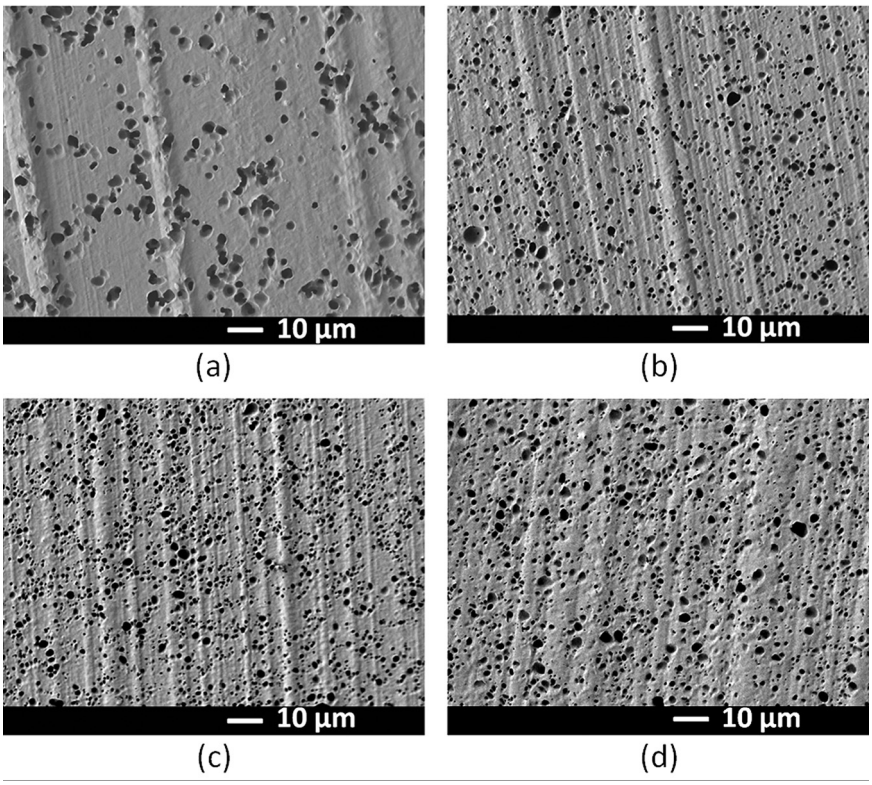

Fig. 9. SEM images of PCL/TPS 80/20 wt% with different carbon nanotube wt% prepared with internal mixer: (a) 0 wt%; (b) 0.5 wt%; (c) 1 wt%; (d) 2 wt%.

carbon nanotubes. The percent crystallinity, however, decreases by incorporating nanotubes for both processes. Like other heterogeneous nucleating agents, the presence of nanofillers has two effects, one is facilitating polymer crystallization due to their nucleating role and the opposite effect due to slower growth and the generation of lamellar defects in the crystalline structure (Grady, 2010). In the case of nanotubes due to their size and molecular level interactions they can interfere more effectively in the growth and forming of spherulites and impose some defects in the crystalline structure.

In a binary blend such as PCL/TPS, the localization of nanotubes determines the extent of nanotube impact on the crystallization. In the extrusion samples of PCL/TPS/nanotubes, the addition of nanotubes decreases the percent crystallinity of PCL and increases crystallization temperature (Table 5), but this change remains at the same level independent of the CNT loading. This is due to the fact that the effect of carbon nanotubes on the crystallization in these samples is limited by its localization at the PCL/TPS interface. Furthermore, as mentioned previously, the droplet size and distribution and consequently the interfacial area remains almost unchanged in the extrusion samples. On the other hand, in the samples prepared by internal mixing where nanotubes were localized in both PCL and at the interface, a significant shift is observed in the crystallization temperature from 0.5 wt% to 1 wt% CNT following a plateau afterwards (Table 5).

Table 5
DSC characteristics of PCL/TPS 80/20 wt% blends with different CNT contents prepared by extruder and internal mixer.

	T_c (°C)	ΔH_c [a] (J/g)	X_c [b] (%)
PCL	26	55.6	40
PCL/TPS[c]	32	56	40
PCL/TPS + 0.5 wt% CNT[c]	35	52	37
PCL/TPS + 1 wt% CNT[c]	35	53	38
PCL/TPS[d]	30	57	41
PCL/TPS + 0.5 wt% CNT[d]	34	52	37
PCL/TPS + 1 wt% CNT[d]	37	51	36
PCL/TPS + 2 wt% CNT[d]	38	51	36

[a] Normalized to PCL unit mass.
[b] $X_c = \Delta H/\Delta H_c^0$, $\Delta H_c^0 = 139$ J/g (Pitt et al., 1981).
[c] Prepared by extrusion.
[d] Prepared by internal mixing.

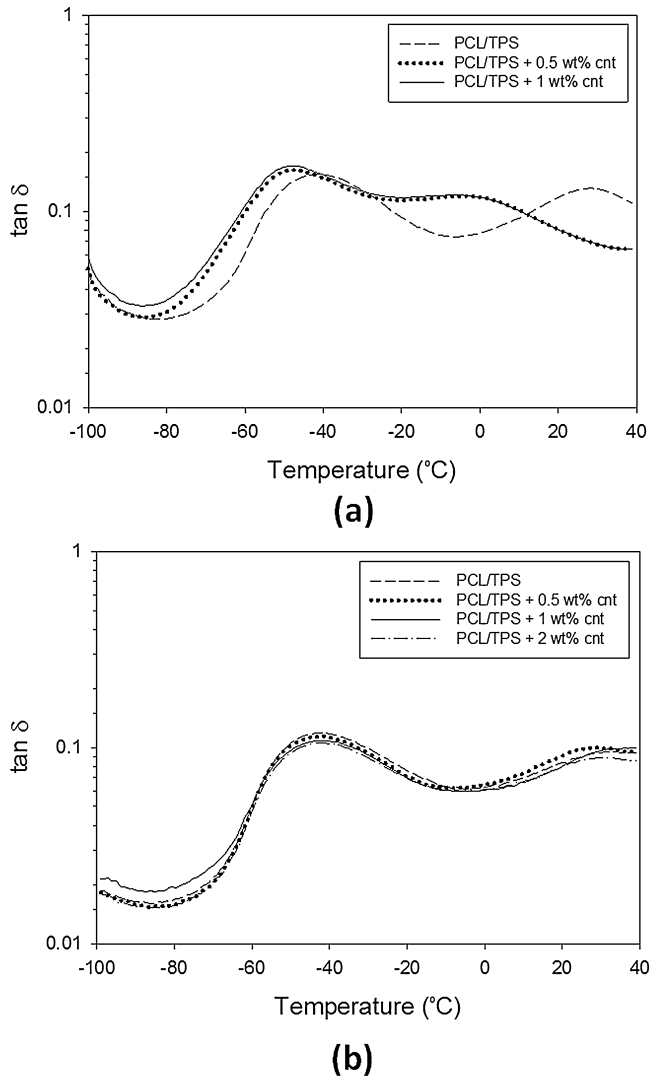

Fig. 10. DMA curves of PCL/TPS 80/20 wt% with different carbon nanotube contents prepared via: (a) extrusion; (b) internal mixer.

3.4. Dynamic mechanical analyses (DMA)

Thermoplastic starch exists as a partially miscible mixture of starch and plasticizer and typically shows two transition peaks in DMA curves. The lower temperature alpha transition, T_α, is attributed to the low molecular weight plasticizer and the higher temperature beta transition, T_β, is for the starch rich domains in TPS (Averous et al., 2000). The addition of carbon nanotubes results in a dramatic temperature reduction (~26 °C) of the starch rich phase transition, T_β, for the samples prepared by extrusion (Fig. 10a). On the other hand, the samples prepared in the internal mixer show no such change (Fig. 10b). In the latter case the nanotubes are localized in the PCL and at the interface, whereas in the case of extrusion a predominant number of the nanotubes are located in the TPS phase.

Some authors have reported an increase in T_g by incorporation of CNTs due to the filler–polymer interaction and a lower degree of chain freedom (Cui, Tarte, & Woo, 2009). However, the opposite effect, i.e. a T_g decrease, has also been frequently reported in the literature (Castillo et al., 2011). The latter effect was mostly attributed to the easier sliding of the polymer chains on the solid surface due to the increased alignment and lower entanglements density in the vicinity of the nanotube surface (Grady, 2011). In the case of carbon nanotubes which are chemically bonded to the starch, pinned starch chains impose orientation and subsequently disentangle from surrounding starch molecules. Some authors have reported that in starch–nanocomposites, nanofillers facilitate starch chain mobility by imposed orientation, decreased entanglement density and interruption of inter-molecular interactions (Gao, Dong, Hou, & Zhang, 2012; Mbey, Hoppe, & Thomas, 2012). Consequently, a lower starch rich phase transition temperature is expected upon localization of the nanotubes in the TPS bulk phase. Also, some other authors have proposed that the slight degradation of polymer matrix in the presence of nanofillers due to the increased viscosity and shear forces might also explain the drop in the transition temperature for starch (Castillo et al., 2011).

4. Conclusions

This work shows that the extrusion melt processing of nanotubes in a PCL/TPS blend results in the nanotubes being located principally in the TPS phase and also at the PCL/TPS interface. This is indicative of a strong driving force particularly when one considers that the nanotubes were first dispersed in the PCL phase. Further static annealing of the blends did not result in any further change in the localization of the nanotubes indicating a stable state of dispersion. Wetting coefficient calculations suggest that the nanotubes will thermodynamically tend to migrate to the PCL/TPS interface. Further investigations via XPS are strongly indicative of the formation of a covalent bond between the carboxylic acid groups on the nanotube surface and the TPS. It was concluded that during dynamic mixing, the nanotubes first move to the interface to minimize the free energy of the system. At the interface a reaction occurs between the carboxylic acid groups of the nanotube and the alcohol groups of the starch and, following this reaction and the formation of a TPS encapsulating layer around the nanotube, the carbon nanotubes are drawn into the thermoplastic starch dispersed phase. Using a different processing technique, the internal mixer, this phenomenon was completely inversed and the nanotubes remained in the PCL phase or at the interface and were not observed in the TPS phase. Further annealing showed an increase presence of nanotubes at the interface, but not in the TPS phase. This result in the internal mixer was attributed to kinetic effects influencing the CNT localization. A rheological analysis indicates the significant shear thinning behavior of TPS. It was concluded that the high viscosity of the TPS phase at the lower shear rates in the internal mixer or during annealing, inhibits the CNT penetration into the starch droplets. This conclusion was confirmed by increasing the processing temperature from 145 °C to 165 °C in the internal mixing process which resulted in the observation of carbon nanotubes in the TPS phase. The results underline the importance of the process and process conditions when adding nanotubes. Carbon nanotubes were found to effectively influence the crystallinity of PCL. It is observed that all of the CNT-incorporated blends of PCL/TPS show a higher T_c than for the neat blend of PCL/TPS which is due to the heterogeneous nucleating effect of carbon nanotubes. The percent crystallinity, however, decreases by incorporating nanotubes for both processes. Like other heterogeneous nucleating agents, the presence of nanofillers has two effects, one is facilitating the crystallization due to their nucleating role and the opposite effect is related to slower growth and lamellar defects in the crystalline structure. DMA analyses were used to investigate the structural changes in the TPS phase. TPS located CNTs were shown to dramatically decrease the starch rich phase transition temperature (~26 °C). This is most likely due to an enhanced sliding of the polymer chains on the solid surface due to the increased alignment and lower entanglement density in the vicinity of the nanotube surface (Cava, Gavara, Lagarón, & Voelkel, 2007; Grady, 2011; Pitt, Chasalow, Hibionada, Klimas, & Schindler, 1981).

Acknowledgments

The authors would like to express their gratitude to TeknorApex Co. for funding this research. The authors would also like to thank Dr. Sepehr Ravati and the polymer blend group for useful discussions. In addition, we would like to thank Ms. Melina Hamdine, Dr. Weawkamol Leelapornpisit and Dr. Josianne Lefebvre at Ecole Polytechnique de Montreal for their effective support in the rheology, TEM and XPS experiments.

References

Abbasi, S., Carreau, P. J., & Derdouri, A. (2010). Flow induced orientation of multiwalled carbon nanotubes in polycarbonate nanocomposites: Rheology, conductivity and mechanical properties. *Polymer*, *51*(4), 922–935.

Angellier, H., Molina-Boisseau, S., Dole, P., & Dufresne, A. (2006). Thermoplastic starch–waxy maize starch nanocrystals nanocomposites. *Biomacromolecules*, *7*(2), 531–539.

Averous, L. (2004). Biodegradable multiphase systems based on plasticized starch: A review. *Journal of Macromolecular Science: Polymer Reviews*, *C44*(3), 231–274.

Averous, L., & Boquillon, N. (2004). Biocomposites based on plasticized starch: Thermal and mechanical behaviours. *Carbohydrate Polymers*, *56*(2), 111–122.

Averous, L., Moro, L., Dole, P., & Fringant, C. (2000). Properties of thermoplastic blends: Starch–polycaprolactone. *Polymer*, *41*(11), 4157–4167.

Bajgai, M. P., Aryal, S., Bhattarai, S. R., Bahadur, K. C. R., Kim, K. W., & Kim, H. Y. (2008). Poly(epsilon-caprolactone) grafted dextran biodegradable electrospun matrix: A novel scaffold for tissue engineering. *Journal of Applied Polymer Science*, *108*(3), 1447–1454.

Bose, S., Bhattacharyya, A. R., Bondre, A. P., Kulkarni, A. R., & Potschke, P. (2008). Rheology, electrical conductivity, and the phase behavior of cocontinuous PA6/ABS blends with MWNT: Correlating the aspect ratio of MWNT with the percolation threshold. *Journal of Polymer Science Part B: Polymer Physics*, *46*(15), 1619–1631.

Bousmina, M., Ait-Kadi, A., & Faisant, J. B. (1999). Determination of shear rate and viscosity from batch mixer data. *Journal of Rheology*, *43*(2), 415–433.

Breuer, O., & Sundararaj, U. (2004). Big returns from small fibers: A review of polymer/carbon nanotube composites. *Polymer Composites*, *25*(6), 630–645.

Castillo, F. Y., Socher, R., Krause, B., Headrick, R., Grady, B. P., Prada-Silvy, R., et al. (2011). Electrical, mechanical, and glass transition behavior of polycarbonate-based nanocomposites with different multi-walled carbon nanotubes. *Polymer*, *52*(17), 3835–3845.

Cava, D., Gavara, R., Lagarón, J. M., & Voelkel, A. (2007). Surface characterization of poly(lactic acid) and polycaprolactone by inverse gas chromatography. *Journal of Chromatography A*, *1148*(1), 86–91.

Ciardelli, G., Chiono, V., Vozzi, G., Pracella, M., Ahluwalia, A., Barbani, N., et al. (2005). Blends of poly-(epsilon-caprolactone) and polysaccharides in tissue engineering applications. *Biomacromolecules*, *6*(4), 1961–1976.

Clark, D. C., Geramita, K., & Baker, W. E. (1999). Investigation of the shear stresses experienced during melting using novel microencapsulated dye sensors. *Journal of Reinforced Plastics and Composites*, *18*(3), 271–278.

Cui, L., Tarte, N. H., & Woo, S. I. (2009). Synthesis and characterization of PMMA/MWNT nanocomposites prepared by in situ polymerization with Ni(acac) (2) catalyst. *Macromolecules*, *42*(22), 8649–8654.

Della Valle, G., Vergnes, B., & Lourdin, D. (2007). Viscous properties of thermoplastic starches from different botanical origin. *International Polymer Processing*, *22*(5), 471–479.

Elias, L., Fenouillot, F., Majeste, J. C., & Cassagnau, P. (2007). Morphology and rheology of immiscible polymer blends filled with silica nanoparticles. *Polymer*, *48*(20), 6029–6040.

Favis, B. D. (2000). Factors influencing the morphology of immiscible polymer blends in melt processing. In D. R. Paul, & C. B. Bucknall (Eds.), *Polymer blends V. 1: Formulation*. Toronto, ON: John Wiley & Sons Inc.

Favis, B. D., Rodriguez-Gonzalez, F. J., & Ramsay, B. A. (2003). Polymer compositions containing thermoplastic starch. US Patent US6605607.

Favis, B. D., Rodriguez-Gonzalez, F. J., & Ramsay, B. A. (2005). Method of making polymer compositions containing thermoplastic starch. U.S. Patent US6844380.

Feng, J., Chan, C.-M., & Li, J.-X. (2003). A method to control the dispersion of carbon black in an immiscible polymer blend. *Polymer Engineering and Science*, *43*(5), 1058–1063.

Fenouillot, F., Cassagnau, P., & Majeste, J. C. (2009). Uneven distribution of nanoparticles in immiscible fluids: Morphology development in polymer blends. *Polymer*, *50*(6), 1333–1350.

Gao, W., Dong, H., Hou, H., & Zhang, H. (2012). Effects of clays with various hydrophilicities on properties of starch–clay nanocomposites by film blowing. *Carbohydrate Polymers*, *88*(1), 321–328.

Goeldel, A., Kasaliwal, G., & Poetschke, P. (2009). Selective localization and migration of multiwalled carbon nanotubes in blends of polycarbonate and poly(styrene-acrylonitrile). *Macromolecular Rapid Communications*, *30*(6), 423–429.

Goeldel, A., Marmur, A., Kasaliwal, G. R., Poetschke, P., & Heinrich, G. (2011). Shape-dependent localization of carbon nanotubes and carbon black in an immiscible polymer blend during melt mixing. *Macromolecules*, *44*(15), 6094–6102.

Goeldel, A., Kasaliwal, G. R., Poetschke, P., & Heinrich, G. (2012). The kinetics of CNT transfer between immiscible blend phases during melt mixing. *Polymer*, *53*(2), 411–421.

Grady, B. P. (2010). Recent developments concerning the dispersion of carbon nanotubes in polymers. *Macromolecular Rapid Communications*, *31*(3), 247–257.

Grady, B. P. (2011). Effects of carbon nanotubes on polymer physics. In *Carbon nanotube–polymer composites, manufacture, properties and applications*. Hoboken, NJ: John Wiley & Sons, Inc.

Grady, B. P. (2012). Effects of carbon nanotubes on polymer physics. *Journal of Polymer Science Part B: Polymer Physics*, *50*(9), 591–623.

Katada, A., Buys, Y., Tominaga, Y., Asai, S., & Sumita, M. (2005). Relationship between electrical resistivity and particle dispersion state for carbon black filled poly (ethylene-co-vinyl acetate)/poly (L-lactic acid) blend. *Colloid and Polymer Science*, *284*(2), 134–141.

Kwok, D. Y., & Neumann, A. W. (1999). Contact angle measurement and contact angle interpretation. *Advances in Colloid and Interface Science*, *81*(3), 167–249.

Li, G., & Favis, B. D. (2010). Morphology development and interfacial interactions in polycaprolactone/thermoplastic-starch blends. *Macromolecular Chemistry and Physics*, *211*(3), 321–333.

Luong, J. H. T., Hrapovic, S., Liu, Y. L., Yang, D. Q., Sacher, E., Wang, D. S., et al. (2005). Oxidation, deformation, and destruction of carbon nanotubes in aqueous ceric sulfate. *Journal of Physical Chemistry B*, *109*(4), 1400–1407.

Ma, X. F., Yu, J. G., & Wang, N. (2008). Glycerol plasticized-starch/multiwall carbon nanotube composites for electroactive polymers. *Composites Science and Technology*, *68*(1), 268–273.

Mbey, J. A., Hoppe, S., & Thomas, F. (2012). Cassava starch–kaolinite composite film. Effect of clay content and clay modification on film properties. *Carbohydrate Polymers*, *88*(1), 213–222.

Moniruzzaman, M., & Winey, K. I. (2006). Polymer nanocomposites containing carbon nanotubes. *Macromolecules*, *39*(16), 5194–5205.

Nair, L. S., & Laurencin, C. T. (2007). Biodegradable polymers as biomaterials. *Progress in Polymer Science*, *32*(8–9), 762–798.

Nuriel, S., Liu, L., Barber, A. H., & Wagner, H. D. (2005). Direct measurement of multiwall nanotube surface tension. *Chemical Physics Letters*, *404*(4–6), 263–266.

Pitt, C. G., Chasalow, F. I., Hibionada, Y. M., Klimas, D. M., & Schindler, A. (1981). Aliphatic polyesters. I: The degradation of poly(ϵ-caprolactone) in vivo. *Journal of Applied Polymer Science*, *26*(11), 3779–3787.

Potschke, P., Pegel, S., Claes, M., & Bonduel, D. (2008). A novel strategy to incorporate carbon nanotubes into thermoplastic matrices. *Macromolecular Rapid Communications*, *29*(3), 244–251.

Queiroz, A. U. B., & Collares-Queiroz, F. P. (2009). Innovation and industrial trends in bioplastics. *Polymer Reviews*, *49*(2), 65–78.

Shahbikian, S. (2010). *Phase morphology development and rheological behavior of non-plasticized and plasticized thermoplastic elastomer blends (Vol. Ph.D.)*. Montreal, Canada: Ecole Polytechnique.

Shin, B. Y., Lee, S. I., Shin, Y. S., Balakrishnan, S., & Narayan, R. (2004). Rheological, mechanical and biodegradation studies on blends of thermoplastic starch and polycaprolactone. *Polymer Engineering and Science*, *44*(8), 1429–1438.

Sumita, M., Sakata, K., Asai, S., Miyasaka, K., & Nakagawa, H. (1991). Dispersion of fillers and the electrical-conductivity of polymer blends filled with carbon-black. *Polymer Bulletin*, *25*(2), 265–271.

Wu, S. (1987). Interfacial energy, structure and adhesion between polymers. In D. R. Paul, & S. Newman (Eds.), *Polymer blends* (vol. 1) (pp. 244–248). New York: Academic Press.

Wu, D., Lin, D., Zhang, J., Zhou, W., Zhang, M., Zhang, Y., et al. (2011). Selective localization of nanofillers: Effect on morphology and crystallization of PLA/PCL blends. *Macromolecular Chemistry and Physics*, *212*(6), 613–626.